Title: Surveillance and Monitoring Program Full-Scale Experiments to Evaluate the Potential for Corrosion in 3013 Containers

Author(s): Narlesky, Joshua Edward; Berg, John M.; Duque, Juan; Harradine, David Martin; Hill, Dallas Dwight; Kaczar, Gregory Michael; Lillard, R. Scott; Lopez, Annabelle Sarita; Martinez, Max Alfonso; Peppers, Larry G.; Rios, Daniel; Romero, Edward L.; Stroud, Mary Ann; Trujillo, Leonardo Alberto; Veirs, Douglas Kirk; Wilson, Kennard Virden Jr.; Worl, Laura Ann

Intended for: Report

Issued: 2017-11-21

Surveillance and Monitoring Program Full-Scale Experiments to Evaluate the Potential for Corrosion in 3013 Containers

JOSHUA NARLESKY, JOHN M. BERG, JUAN DUQUE, DAVID M. HARRADINE (RETIRED), DALLAS HILL, GREG KACZAR, R. SCOTT LILLARD, ANABELLE LOPEZ, MAX A. MARTINEZ (RETIRED), LARRY PEPPERS, DANIEL RIOS, EDWARD ROMERO, MARY ANN STROUD, LEONARD TRUJILLO (RETIRED), D. KIRK VEIRS, KENNARD WILSON, LAURA A. WORL

NOVEMBER 2017

Abstract

A set of six long-term, full-scale experiments were initiated to determine the type and extent of corrosion that occurs in 3013 containers packaged with chloride-bearing plutonium oxide materials. The materials were exposed to a high relative humidity environment representative of actual packaging conditions for the materials in storage. The materials were sealed in instrumented, inner 3013 containers with corrosion specimens designed to test the corrosiveness of the environment inside the containers under various conditions. This report focuses on initial loading conditions that are used to establish a baseline to show how the conditions change throughout the storage lifetime of the containers.

Introduction

The Department of Energy (DOE) has established a surveillance program[1] to assure that plutonium-bearing materials stabilized and packaged according to the DOE Stabilization, Packaging, and Storage Standard (DOE-STD-3013)[2] can be stored safely for 50 years. The surveillance program combines field surveillance of packaged 3013 containers currently in the storage population with shelf-life experiments to evaluate the Packaging and Storage Standard. Shelf-life experiments consist of small-scale and full-scale experiments aimed at providing information on gas generation or corrosion concerns that may be observed in the storage population. Although shelf-life experiments have demonstrated that the packaged 3013 containers can safely handle the pressure generated by material packaged at the bounding conditions of the DOE-STD-3013, these experiments have also demonstrated that stress corrosion cracking (SCC) can occur under conditions allowed by versions of DOE-STD-3013 prior to 2012.[3,4] The shelf-life experiments test the bounding conditions, and it is expected that the observed gas generation and corrosion are more severe than observations made on the storage population. Destructive examinations of 3013 containers in the storage population have consistently shown that the observed corrosion is much less severe. Because the conditions of the packaged materials in the storage population do not approach the bounding conditions for the DOE-STD-3013, a test plan was developed to determine the conditions under which SCC occurs with respect to various known parameters in the stabilization and packaging process.[5] The original test plan was subsequently revised to include additional studies to investigate localized corrosion occurring near inner container closure welds and to assess whether through-wall corrosion of a 3013 inner container via stress corrosion cracking (SCC) near the closure weld would be credible during storage.[6]

The original SCC test plan included full-scale plutonium oxide studies at Los Alamos National Laboratory (LANL) aimed at determining the influence of loading conditions inside the 3013 containers on the resulting storage conditions and the corrosion that occurs during storage.[5] These full-scale tests investigate the effect of the loading conditions using plutonium oxide materials with specific amounts of chloride salts. These materials were exposed to a controlled, high-relative humidity environment that is representative of the packaging conditions at Hanford and considered bound of the packaging conditions at other sites. Corrosion specimens were placed inside the test containers for future examination. The materials were then loaded into instrumented 3013 inner containers for storage. The stored containers were continuously monitored to provide the container pressure, temperature, and relative humidity. The results of these experiments will help answer the following questions:

- What is the effect of the individual chloride salt components on storage conditions?
- What is the relative humidity in the packaged 3013 and how does it change over time?
- Does corrosion occur under storage conditions?
- What type(s) of corrosion occurs under these conditions (general corrosion; pitting corrosion, and/or stress corrosion cracking)?
- Where does corrosion occur within containers?

This report describes the test materials, the loading conditions inside the glovebox, and the initial conditions inside the containers during the first 30 days of storage. These conditions can be used to establish a baseline to show how the conditions change throughout the storage lifetime of the containers.

Background

Chloride Salt Components

The chloride salt components in the packaged materials responsible for the corrosion of the 3013 storage containers are chlorides of magnesium or calcium. These components, referred to as alkaline earth chlorides (AEC) in this report, form aqueous chloride solutions within the range of relative humidity measured inside packaging gloveboxes.[7] Corrosion may occur in the contact region of the container when small amounts of electrolyte (liquid phases), formed by the deliquescence of the chloride salt components, react with the container. The relative humidity and temperatures at which the various salt components form crystalline hydrates are given in Table 1, along with the deliquescence relative humidity (DRH), or the relative humidity at which salt forms an aqueous solution.

Sodium and potassium chloride do not form crystalline hydrates and do not deliquesce under packaging or storage conditions. Chlorides of calcium are likely in the form of potassium calcium chloride ($KCaCl_3$), which is commonly referred to as chlorocalcite, or a calcium chloride hydrate ($CaCl_2{\cdot}xH_2O$). Chlorocalcite is formed when calcium chloride and potassium chloride are mixed together and heated above the melting temperatures of both salts. As shown in Table 1, this compound deliquesces at 16% relative humidity and does not form crystalline hydrates. Therefore, one can expect liquid phases to form under packaging conditions when the relative humidity is above 16%. Any calcium chloride hydrates in the material will deliquesce between 16 and 29% relative humidity. Chlorides of magnesium are likely in the form of potassium magnesium chloride ($KMgCl_3$), which is commonly referred to as carnallite when in its hydrated form ($MgCl_2{\cdot}6H_2O$). Potassium magnesium chloride is formed when magnesium chloride and potassium chloride are mixed together and heated above the melting temperatures of both salts. Moisture sorption on anhydrous $KMgCl_3$ occurs when the relative humidity is greater than 2% and results in the formation of the hexahydrate. The hexahydrate form deliquesces at between 50 and 57% relative humidity depending on the temperature of the material. Any magnesium chloride hydrates in the material will deliquesce between 27 and 33% relative humidity.

Table 1. Equilibrium relative humidity for chloride salts, solutions and crystalline hydrates.

Deliquescence Relative Humidity (RH) of Major Salt Components				
	Ref No.	**%RH at 25ºC**	**%RH at 50ºC**	**%RH at 70ºC**
KCl	8	84	81	79
NaCl	8	75	74	76
$KMgCl_3\cdot 6H_2O$	n/a	57	54	50
$MgCl_2\cdot 6H_2O$	8	33	31	27
$CaCl_2\cdot 6H_2O$	9	29		
$CaCl_2\cdot 4H_2O$	9	21[†]	17 (at 44ºC)	
$KCaCl_3$	7	16[†]	19[†]	21[†]
$CaCl_2\cdot 2H_2O$	10	16[†]	17	18
Minimum Relative Humidity (RH) for Hydrate Formation				
		%RH at 25ºC	**%RH at 50ºC**	**%RH at 70ºC**
$CaCl_2\cdot 6H_2O$	11	21		
$CaCl_2\cdot 4H_2O$	11	9 (13[†])	14 (at 44ºC)	
$MgCl_2\cdot 6H_2O$	11	3	5	7
$CaCl_2\cdot 2H_2O$	11	4 (2[†])	5	7
$KMgCl_3\cdot 6H_2O$	7	2[†]	2[†]	2[†]
$MgCl_2\cdot 4H_2O$	11	0.2	0.4	0.8
$MgCl_2\cdot 2H_2O$	11	0.04	0.1	0.2

[†] Indicates values measured/reproduced [7]
Shading indicates that data is unavailable because the hydrate decomposes at the given temperature.

Storage and Packaging Conditions

At the time Hanford, Rocky Flats, and Savannah River Site were packaging material for storage in 3013 containers, DOE-STD-3013 required oxides to be stabilized by heating to 950°C for a minimum of 2 hours.[3,4] However, an equivalency allowed chloride-bearing oxides to be stabilized at 750°C to reduce damage to the stabilization furnaces.[12] The standard also required the moisture content of the material to be determined by an approved method (thermogravitational analysis, loss on ignition, etc.) and be less than 0.5 wt%. Following stabilization, the oxide could be staged, then packaged within several days, provided that the moisture content remained below 0.5 wt%.

It was believed that controlling the moisture levels below the 0.5 wt% limit set by the DOE standard would minimize the risk of the adsorbed moisture leading to corrosion. Therefore, controlling relative humidity in the 3013 packaging gloveboxes was not required by the packaging sites under the 2000 and 2004 versions of DOE-STD-3013. Lawrence Livermore, Los Alamos, and Rocky Flats packaged under dry conditions, which were normal operating conditions in those facilities; but the packaging gloveboxes at Savannah River and Hanford did not use dry air and experienced much higher humidity. Relative humidity measurements indicated that the C-Line glovebox humidity ranged from 14 to 56% during packaging. The materials being packaged in C-Line were exposed to the humid atmosphere for a time period ranging from several hours to several days. These relative humidity levels are greater than the DRH for the calcium chloride and the magnesium chloride salts and allow the formation of liquid phases in the material matrix that may persist in the material after packaging in the 3013 container.

Figures 1 and 2 compare the glovebox conditions at the packaging sites with the DRH of the AEC salt components. The blue lines in Figure 1 show the relative humidity levels at which the calcium chloride salts form liquid phases. Chlorocalcite is believed to be the predominant calcium chloride phase in the packaged materials because potassium chloride in the material (typically in concentrations of an order of magnitude greater than the calcium chloride[13]) would react with calcium chloride to form this compound during stabilization. The colored bands in Figure 1 indicate the range of relative humidity at the glovebox temperature and inside a pan holding material. The relative humidity at various temperatures inside the material was calculated, based on relative humidity measurements taken at the ambient glovebox temperature, assuming the water vapor pressure is constant throughout the glovebox and material. Materials with calcium chlorides are likely to have liquid phases forming in cooler regions as well as in warmer regions of the material under the packaging conditions at Hanford. Therefore, the band representing the Hanford C-line glovebox relative humidity is shown in red in Figure 1. The band representing the Savannah River FB-Line gloveboxes is shown in yellow because the relative humidity is sufficiently high for liquid phase formation on the surface of the material, but the higher temperatures near the center of the material would limit the formation of liquid phases. The bands for Los Alamos and Lawrence Livermore glovebox lines are shown in green because liquid phases are not likely to form in the materials packaged at these sites.

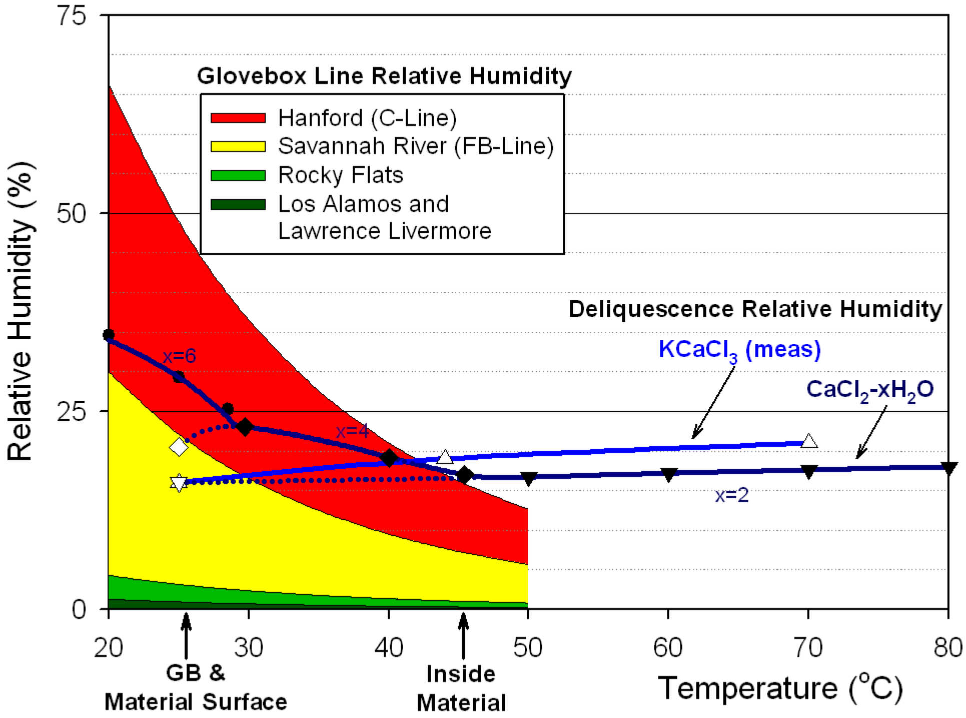

Figure 1. Comparison of the temperature dependent DRH for calcium chlorides (curves) and glovebox line relative humidity at each of the packaging sites represented by the colored bands. Estimates of the relative humidity at higher temperatures were obtained from the glovebox relative humidity measurements or set points at room temperature.

The blue lines in Figure 2 show the relative humidity levels at which the magnesium chloride salts form liquid phases. Materials with magnesium chlorides are likely to have liquid phases forming in cooler regions as well as in warmer regions of the material under the packaging conditions at Hanford. Therefore, the band representing the Hanford C-line glovebox relative humidity is shown in red in Figure 2. Although $KMgCl_3$ is the predominant magnesium chloride phase in the packaged material, liquid phases may form throughout the material if small amounts of $MgCl_2$ are also present. Materials with magnesium chloride salts packaged at the other sites and exposed to lower relative humidity at packaging would not have the same risk for liquid phase formation. Therefore, the bands representing the relative humidity in the packaging gloveboxes at the other sites are shaded green.

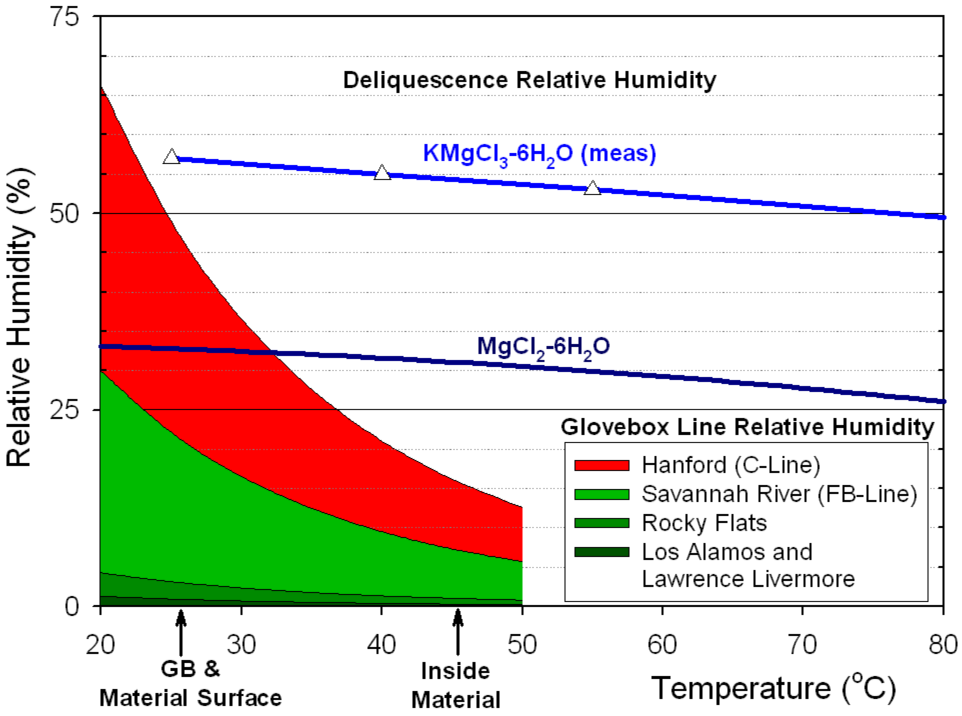

Figure 2. Comparison of the temperature dependent DRH for magnesium chlorides (curves) and glovebox line relative humidity at each of the packaging sites represented by the colored bands. Estimates of the relative humidity at higher temperatures were obtained from the glovebox relative humidity measurements or set points at room temperature.

While the conditions in the Hanford C-line and the Savannah River FB-line gloveboxes support liquid phase formation during packaging, the presence of liquid phases and the extent to which they form depends on the exposure time of the material to moisture during packaging and the salt concentration in the material. Materials with low concentrations of AEC salt components require less exposure time to reach deliquescence than materials with higher concentrations of AEC salt components. Additionally, the effect of thermal gradients must be considered. The water vapor pressure inside the packaged 3013 is controlled by the solution or the salt hydrate phase that is formed when the material is exposed to moisture. Thermal gradients drive moisture from warmer regions (typically near the material center line) to cooler regions (typically along the container walls). This results in higher relative humidity in cooler regions and lower relative humidity in the warmer regions. The increased relative humidity in the cooler regions of the container may result in the formation of liquid phases even though the overall moisture to salt ratio may be below what is required for deliquescence.

Experimental

The test materials in this experiment included six full-scale batches of material containing a mixture of plutonium oxide and chloride salts, designed to simulate scrap material generated by the electrorefining process. These test materials include the following:

I. **Base Material:** 75.8 wt% Pu with sodium and potassium chloride salt impurities.
II. **Low Ca test material:** Base Material with 0.34 wt% $KCaCl_3$
III. **Low Mg test material:** Base Material with 0.34 wt% $KMgCl_3$
IV. **High Ca test material:** Base Material with 3.4 wt% $KCaCl_3$
V. **High Mg test material:** Base Material with 3.4 wt% $KMgCl_3$
VI. **PMAXBS test material:** 74 wt% Pu with sodium and potassium chloride salt impurities. (Analytical chemistry indicates that 0.016% soluble Mg and 0.006% soluble Ca are present.)

Test materials I through V in this experiment were designed to be chloride-containing plutonium oxides having approximately 75 wt% Pu (86% PuO_2). Test materials II through V have AEC salt components added to the material. The amount of added salt was selected so that the salt in containers II and III would have greater than six waters of hydration with the addition of 0.5 wt% moisture (high relative humidity), and the salt in containers IV and V would have less than six waters of hydration with the addition of 0.5 wt% moisture (low relative humidity). Test material VI is PMAXBS, which was loaded in previous full-scale tests and was found to cause corrosion. (A brief history of the previous full-scale loadings is given in Appendix 1.) This test material was included in the current set of experiments as a positive control.

To reproduce the packaging conditions and storage conditions, the test materials were exposed to a controlled, high relative humidity environment until the moisture sorption reached the 0.5 wt% limit or until the AEC salt components in the material reached saturation below the 0.5 wt% moisture limit. The materials were then placed into instrumented 3013 test containers. Insulation was placed around the containers to simulate warm storage conditions in a vault or in a shipping container. The container pressure, relative humidity, temperature were continuously monitored, and gas sampling was done to ensure that hydrogen and oxygen produced by radiolysis of the adsorbed moisture did not result in a flammable mixture of gases inside any of the containers.

Preparation of the Test Materials

Preparation of test materials I-V occurred in the following steps. First, the Base Material was prepared and stored in hermetically-sealed conflat containers. Second, the AEC salt mixture was prepared in a non-radiological, inert glovebox. Then, the AEC salt mixture was transferred in a hermetically-sealed container (used to limit moisture sorption) to the dry air, radiological glovebox where it was mixed with the Base Material. Next, the test materials were processed in the Turbula® mixer for one hour. Finally, the test materials were exposed to a humidified atmosphere to simulate the packaging conditions at Hanford.

Preparation of the Base Material

The Base Material for containers I-V contains 75.8 wt% Pu (86% PuO_2) with the remainder mostly sodium and potassium chloride. The Base Material was prepared from the Modified Masterblend (MMB), which was intended for use in previous full-scale experiments (See Appendix 1). The magnesium chloride in the MMB was removed by heating the MMB material in the presence of moisture, which hydrolyzes the magnesium chloride to form magnesium oxide and hydrogen chloride gas. Moisture was added to the air inside the furnace by heating the MMB material simultaneously with kaolin, a mineral which releases hydration waters at specific temperatures. The MMB material was split into batches and placed in a furnace. Small dishes of Kaolin (50 to 100 g) were placed on top of the MMB material. The kaolin and MMB materials were calcined in air simultaneously according to the following profile to maximize the desorption of water from the kaolin to react with the magnesium chloride: 450°C for 1 hour; 480°C for 2 hours; 510°C for 2 hours; and 540°C for 1 hour. After heating, the resulting material, free of magnesium chloride, was removed from the furnace and stored in hermetically-sealed conflat containers.

Preparation of AEC Salt Mixtures

Two chloride-salt mixtures were prepared to spike the Base Material with the AEC: a $CaCl_2$-KCl mixture and a $MgCl_2$-KCl mixture. These salt mixtures were prepared from reagent grade KCl, anhydrous $MgCl_2$ (Alfa-Aesar, 99.9%, sealed in glass ampoule), and anhydrous $CaCl_2$ (Alfa-Aesar, 99.9%, sealed in glass ampoule). The individual salts were measured and mixed in non-radiological, inert glovebox (O_2 concentration less than 10 ppm; dew point less than -70°C) according to the compositions given in Table 2. Potassium chloride was added to both mixtures in 10% excess to ensure complete reaction of the AEC component to form the fused salt compound. The salts were ground together with a mortar and pestle, poured into a porcelain crucible, and placed in the furnace. The $CaCl_2$-KCl mixture was heated to 800°C in 30 minutes, maintained at temperature for 30 minutes, and cooled to about 40°C. The $MgCl_2$-KCl mixture was heated to 850°C in 30 minutes, maintained at temperature for 30 minutes, and cooled to about 40°C in the furnace. The salt was then removed from the crucible, ground with a mortar and pestle, and stored in a hermetically-sealed container until used.

Table 2. Composition of salt mixtures added to Base Material.

Salt Mixture	Fused Salt Compound	Salt Species	wt%
$CaCl_2$-KCl	$KCaCl_3$	$CaCl_2$	57.5
		KCl	42.5
$MgCl_2$-KCl	$KMgCl_3$	$MgCl_2$	53.7
		KCl	46.3

Processing of Test Materials

Processing of the test materials was done in a dry air, radiological glovebox (relative humidity < 1%). For each of the test materials I through V, 2,400 to 2,500 grams of the Base Material were poured into a Turbula® mixing container with 1-cm diameter ceramic beads. The weight of the Base Material was chosen so that the total weight of the Base Material and the salt mixture was 2,500 grams. The salt mixture (if used) was added to the Base Material inside the mixer in the proportions given in Table 3. The lid was then placed on the mixing container and sealed in place with tape. The contents of the mixing container were shaken for 1-hour with the Turbula® system. After mixing, the material was poured through a screen to remove the ceramic beads and placed in a hermetically-sealed conflat container.

Table 3. Test materials for SCC experiment with the respective concentrations of added salt, concentrations of desired salt compound ($KCaCl_3$ or $KMgCl_3$), and concentrations of AEC salt components.

No.	Test Material	Added Salt Mixture	Target Salt Concentration (wt%)	Concentration of XCl_2-KCl (wt%)	AEC (calculated) (wt%)	Soluble AEC Cation (ppm)
I	Base	None	0.00	0.00	0.00	None
II	Low Ca	$CaCl_2$-KCl	0.34	0.32	0.19	Ca: 700
III	Low Mg	$MgCl_2$-KCl	0.34	0.33	0.18	Mg: 470
IV	High Ca	$CaCl_2$-KCl	3.4	3.22	1.93	Ca: 7,000
V	High Mg	$MgCl_2$-KCl	3.4	3.00	1.69	Mg: 4,300

Processing of PMAXBS

Test material VI, PMAXBS, was produced by the MIS program to represent Rocky Flats oxide generated in pyrochemical processes. It was made by blending LANL-produced oxide in the form of burned anode heel with low-purity residue from the electrorefining process containing magnesium chloride.[14] The composition of the PMAXBS test material is given in Table 4.

Table 4. Plutonium concentration and composition of the Chloride-Salt Components in the PMAXBS test material.

Pu wt%	71.8
Cl ppm (total)	52,000
Cl ppm (leach)	62,000*
Mg ppm (total)	2,400
Mg ppm (leach)	200
Ca ppm (total)	200
Ca ppm (leach)	60
Na ppm (total)	19,000
Na ppm (leach)	19,000
K ppm (total)	35,000
K ppm (leach)	27,000
*The difference between total Cl and soluble Cl is attributed to material inhomogeneity and sampling.	

Test material VI, PMAXBS, was used in four previous full-scale experiments. Upon completion of the fourth full-scale experiment with 0.4 wt% added moisture, the material was placed in a large boat and heated on a hot plate to remove the moisture. Thermocouples (TC) were placed under the boat and inside the material. The hot plate was powered on for two hours, and the material TC reached 200°C. The hot plate was then powered off, and the material was allowed to cool in the dry glovebox atmosphere. The hot plate was turned on again for two hours, then allowed to cool in the dry glovebox. The material was weighed and then stored until it was used in these experiments.

Moisture Addition and Loading

Moisture was added to each of the test materials by exposing them to a high relative humidity environment inside an enclosure (see Figure 3). The conflat containers were emptied into a stainless steel Vollrath pan (20.75 x 12.75 in), and the pan with the material was placed on the balance inside the enclosure. A sodium bromide saturated solution (DRH=57.8% relative humidity at 25°C) was placed in a shallow dish near the front-right corner of the enclosure (see Figure 3b), and the enclosure was sealed with tape. The sodium bromide solution was expected to maintain the relative humidity inside the enclosure between 50 and 55% at room temperature, based on measurements made with the enclosure empty.

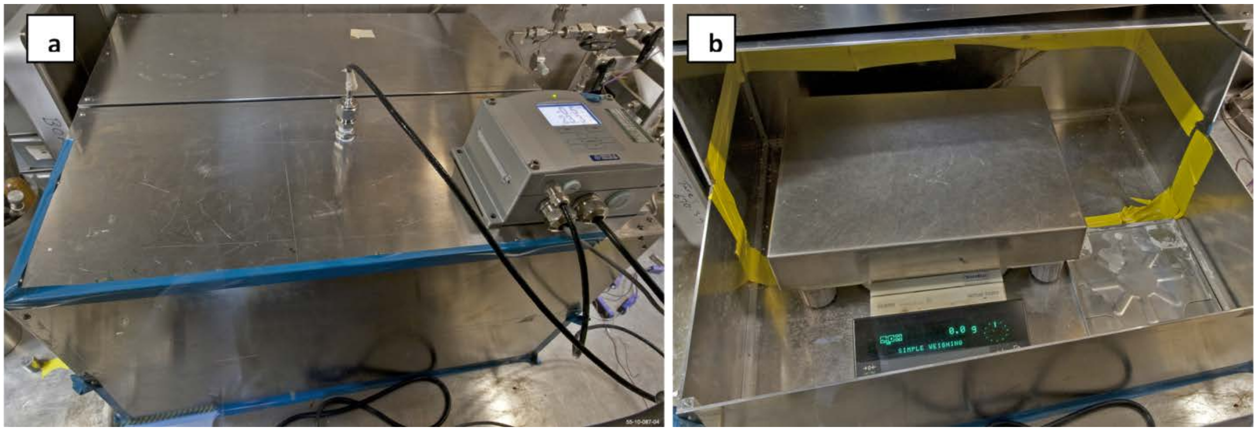

Figure 3. Enclosure used to reproduce the high relative humidity environment experienced by materials packaged in Hanford C-Line gloveboxes. (a) Outside of enclosure with lid closed. (b) Inside of enclosure with lid removed.

The relative humidity and temperature of the enclosure were measured with a Vaisala HMT330 series humidity and temperature sensor and transmitter. Thermocouples were also placed inside the material, under the metal pan, and inside the NaBr solution to measure the temperatures at these locations. Temperature, relative humidity, and the mass of the material were recorded for the entire time the material was inside the enclosure. The material was removed from the enclosure when the total adsorbed moisture reached the target concentration of 0.5 wt%, which is maximum amount of moisture allowed by DOE-STD-3013, or at an equilibrium concentration below 0.5 wt%.

The total adsorbed moisture was determined by adding the initial moisture on the material (as it was received from the vault) to the moisture adsorbed by the material while inside the enclosure. A small sample (1 to 10-g) was obtained from the material prior to placing exposure to the high relative humidity inside the enclosure. The initial moisture was determined by measuring the weight loss of small samples (1 to 10-g) heated in a 200°C furnace for two hours or by obtaining TGA measurements on the samples.

After exposure to a high relative humidity environment, the test materials were immediately placed in instrumented 3013 inner containers by pouring the material through the threaded hole in the lid. The cap containing burst disk was then installed and sealed to the container lid with an O-ring. The containers were installed on the large-scale array, and insulation was placed around each container to simulate the warmer conditions encountered during storage. The container pressure, headspace relative humidity and the temperature at various locations in the container were monitored throughout the experiment. The gas composition inside the containers was determined by gas chromatography to ensure that the gas mixture inside the container does not become flammable.

Container and Corrosion Tree

Each container included a corrosion tree (Figure 4) with various specimens that aid in determining the type of corrosion supported by the environment inside the container during storage. Table 5 lists each container along with the corrosion test specimens installed on each corrosion tree. Crevice corrosion is investigated through the use of crevice specimens and lid section specimens, both of which are colored red in Figure 4. The crevice specimen consists of two flat pieces of metal, bolted together. The lid section specimens consist of a one-eighth section cut from a welded 3013 inner container lid and sidewall. A crevice exists where the sidewall and lid meet. Stress corrosion cracking is investigated through the use of double cantilever beam (DCB) specimens (yellow) and teardrop specimens (gray). The teardrop specimens consist of two flat pieces of metal that were welded together and bent into the shape of a teardrop. The DCBs consist of two parallel beams joined at one end. A small crack is initiated between the beams at the open end, and a wedge is placed between the beams to maintain the stress at the crack location. The DCBs are electronically monitored during the experiment to measure growth of the crack through changes in resistance. The DCBs in the headspace region had a small droplet of calcium chloride applied to the crack at the time of loading.

The corrosion trees were assembled, cleaned, and placed in the cleaned, modified 3013 inner containers. The container lids were then laser welded to the container bodies. The assembled containers were then introduced into the glovebox line and moved to the location for material loading.

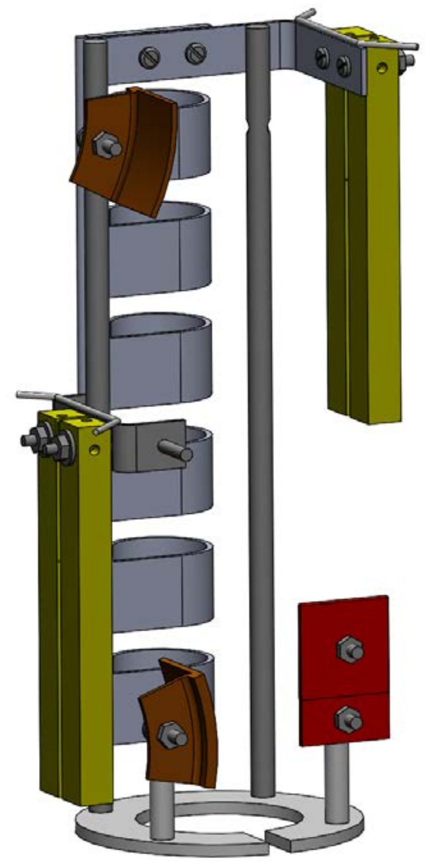

Figure 4. Diagram of a corrosion tree consisting of one crevice specimen, two lid section specimens, two DCB specimens, and six teardrop specimens.

Table 5. Table of test containers with their corresponding corrosion test specimens, materials of construction, and locations on the corrosion tree.

Test Material:	**I** **Base Material**	**II** **Low Ca**	**III** **Low Mg**	**IV** **High Ca**	**V** **High Mg**	**VI** **PMAXBS**
Container ID / Material of Construction:	FTP0002 316L	FTP0014 316L	FTP0009 316L	FTP0010 316L	FTP0003 316L	FTP0013 316L
Crevice	None	ACA-5 (316L)	ACA-6 (316L)	ACA-7 (316L)	ACA-8 (316L)	ACA-4 (316L)
DCB: (HS) † (CR)	None	04-TL-05 (304L) 04-TL-16 (304L)	16-LT-9 (316L) 16-LT-6 (316L)	04-LT-7 (304L) 04-LT-5 (304L)	04-TL-17 (304L) 04-TL-15 (304L)	16-LT-7 (316L) 04-LT-4 (304L)
Lid Section: (HS) (CR)	None	SRS: 5-2 SRS: 5-1	Hanford: 6-2 Hanford: 6-1	Hanford: 7-1 Hanford: 7-2	SRS: 8-1 LLNL: 8-2	SRS: 4-1 SRS: 4-2
Teardrops: (listed top to bottom)	304L 01, 03, 04, 05, 06, 07	316L 07, 06, 05 03, 02, 01	316L 15, 14, 13, 12, 11, 10	304L 19, 20, 21, 22, 23, 24	304L 30, 29, 28, 27, 26, 25	304L 08, 09, 10, 13, 14, 15
† $CaCl_2$ applied to crack tip of 304L specimens in the headspace region.						
HS: headspace CR: contact region						

Results and Discussion

Humidity Control

The atmosphere in the glovebox line where the test materials are handled is maintained by the facility at very low relative humidity (typically -20°C dew point) under normal conditions. Therefore, a humidified enclosure was used to expose the test materials to a constant relative humidity between 50 and 55%. The relative humidity inside the enclosure was controlled by a saturated solution that continually supplies moisture to the air inside. In order to maintain a constant relative humidity, the solution must be capable of supplying moisture to the atmosphere at a rate faster than both the sorption rate of the material and the rate at which the moisture escapes the enclosure.

Two test runs were completed prior to using the enclosure in these experiments. One test run was done to determine the length of time required for the enclosure to reach the desired relative humidity of 50 to 55% while the enclosure was empty, and the other test was done to determine the maximum rate that the solution can provide moisture. In the first test, a shallow pan filled with saturated sodium bromide solution was placed on the balance inside the sealed enclosure. The results indicated that the enclosure reached 50% relative humidity in approximately 5 hours when empty and required 2.1 g of water. The solution supplied moisture at a rate of 0.4 to 0.8 g/hr until the enclosure reached 50% relative humidity. After the enclosure reached steady state, the solution supplied moisture at 0.14 g/hr to maintain the relative humidity around 55%. These results show the baseline operating conditions of the enclosure and provide a leak rate for the system of 0.14 g/hr. In the second test, the maximum evaporation rate of the solution was determined by placing saturated sodium bromide solution in the solution pan and leaving the enclosure open to the glovebox atmosphere. During this experiment, the glovebox relative humidity remained dry (less than 1% relative humidity), and the evaporation rate of the solution was 1.25 g/hr.

Figure 5 shows the relative humidity as a function of time for the empty enclosure and for each of the test materials. The relative humidity reached steady state in approximately 8 to 10 hours when it was empty. The PMAXBS test material, which has very little AEC, also reached steady state in approximately 8 to 10 hours. (Due to an issue with the data acquisition system, the relative humidity data was not saved during the exposure of the Base Material; however, the relative humidity throughout the exposure is presumed to be similar to what was measured with the enclosure empty.) The relative humidity measured in the enclosure during the exposure of the Low Ca and the Low Mg test materials reached steady state in about 10 to 15 hours. The relative humidity measured in the enclosure during the exposure of the High Ca and the High Mg test materials did not reach steady state. This was due to the higher concentrations of AEC salt components in these materials resulting in higher rates of moisture sorption by the material.

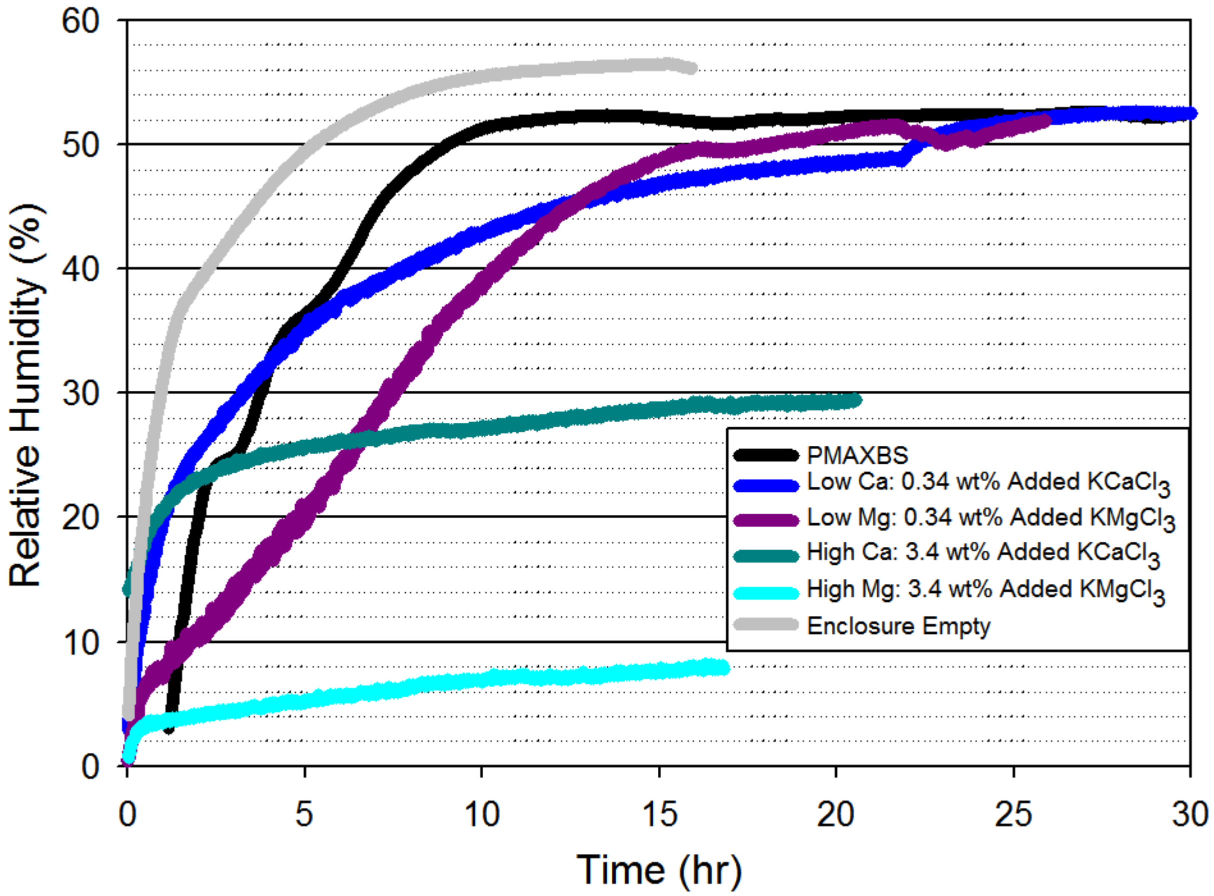

Figure 5. Relative humidity inside the enclosure during moisture addition. The gray curve shows the typical relative humidity rise while the enclosure is empty. (Data are not available for the Base Material due to a failure data collection system.)

Moisture Addition and relative humidity

The curves in Figure 6 show the amount of moisture adsorbed on the test materials as a function of exposure time. We speculate that the details in these curves can be explained as follows. The black line shows the moisture sorption for the PMAXBS test material, which had a weight gain of 0.07 wt% moisture. The Base Material (not shown) was exposed to similar conditions and experienced a weight gain of 0.04 wt%. The moisture adsorbed on the Low Ca and Mg test materials reached equilibrium with the moisture in the enclosure at concentrations of 0.28 and 0.29 wt%, respectively. Because these materials have lower concentrations of AEC salt components, the effect of thermal gradients in the material become more apparent. Initially, rapid moisture sorption occurred due to adsorption by the AEC salt components near the surface of the material, which was cooler and had a higher relative humidity than the center of the material. Once the surface reached saturation, moisture sorption stopped or slowed until relative humidity in the center of the material increased to levels that allow further sorption. For example, the moisture sorption on the Low Ca test material stopped at 0.09 wt%. When the moisture sorption resumed, the relative humidity calculated at the bottom of the pan had reached 15%.

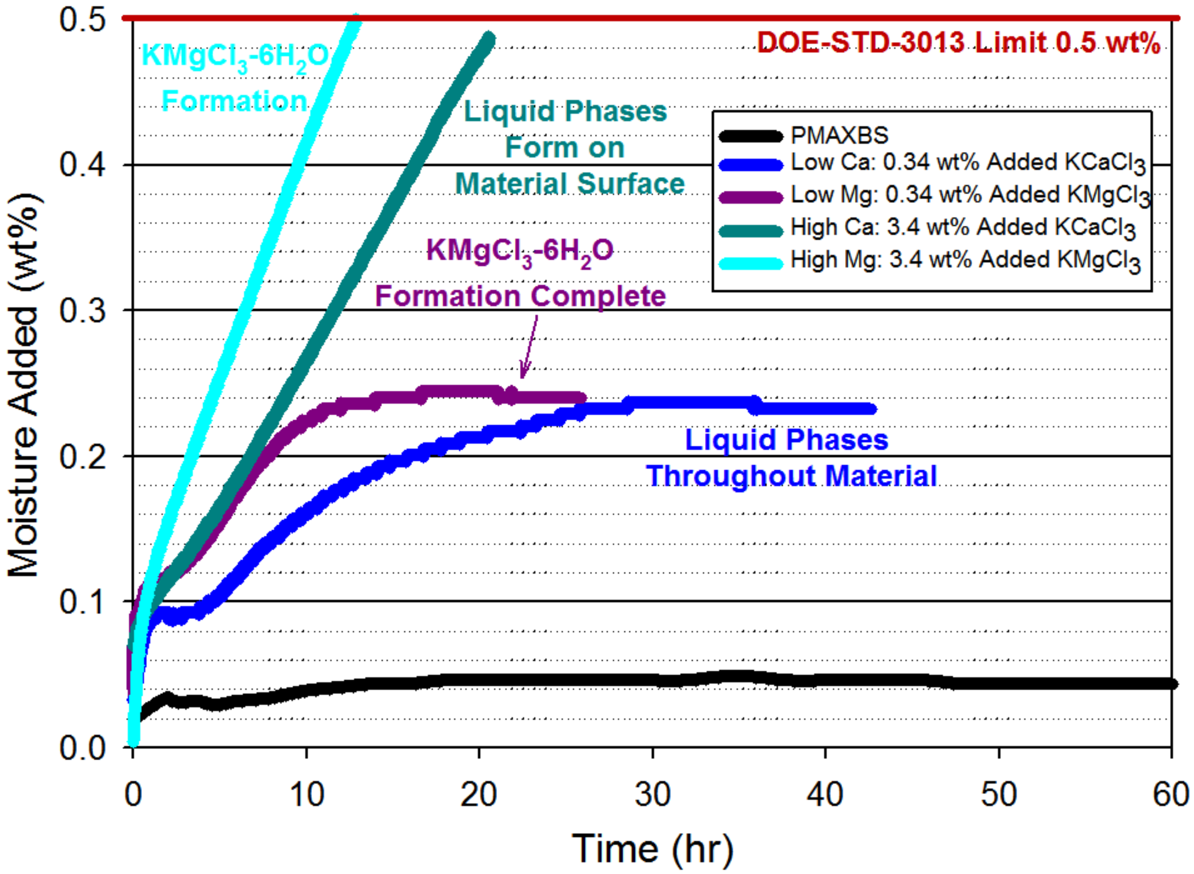

Figure 6. Moisture addition as a function of time for each test material. The measurements for added moisture in this plot are for illustrative purposes only. The amounts of adsorbed moisture shown here may be affected by TCs positioned within the material. Accurate measurements of the adsorbed moisture obtained by weighing the material without the TCs are given in Table 6. (Data are not available for the Base Material due to a failure data collection system.)

The High Mg and High Ca test materials had the fastest sorption rates. The moisture adsorbed on these materials did not reach equilibrium with the moisture in the enclosure. We speculate that most of the moisture adsorption occurred near the surface of the material. The nearly constant rate of moisture adsorption indicates that saturation did not occur. The High Mg test material reached the 0.5 wt% moisture limit in 12 hours and was removed from the enclosure. The maximum relative humidity measured in the enclosure during the exposure of the High Mg test material was measured to be 8%. This relative humidity was below the DRH for the AEC salt component in the material; therefore, the formation liquid phases was not expected. The High Ca test material was removed from the enclosure after 21 hours to avoid exceeding the 0.5 wt% moisture limit. The relative humidity was above the DRH for the AEC salt component for most of the exposure period, so we infer that liquid phases were being formed. Upon removing the material from the enclosure, it was noted that the top layer of the material in the pan had a darker appearance than the material beneath the surface, which indicates an uneven distribution of moisture.

Table 6 gives the final moisture value in wt% for each of the test materials after exposure to moist air inside the enclosure. The final moisture is calculated as the sum of the added moisture and the initial moisture on the material. The initial moisture was determined either by measuring the weight loss from a sample of the material after it was heated to 200 °C in the furnace or by TGA. The initial moisture for the Low Mg test material was not measured. However, the handling conditions and the concentrations of AEC salt components in both the Low Ca and Low Mg test materials were the same, so the initial moisture was estimated to be the same as the initial moisture measured on the Low Ca test material.

The ratio of the water to metal cation was calculated from the total added moisture and the total amount of the AEC salt component added to the material. Generally, liquid phases are expected to form when the ratio of the water to metal cation is greater than six. Therefore, the conditions in the enclosure allowed the AEC salt components in the Low Ca and Low Mg test materials to adsorb greater than 6 waters of hydration and to deliquesce. The High Ca and High Mg test materials have water to metal cation ratios less than six, which suggests that liquid phases would be unlikely. However, $KCaCl_3$ can deliquesce directly without prior formation of hydrates when the RH reaches 16%, making it possible to form a liquid phase without forming solid crystalline hydrates.

Table 6. Results for moisture addition on the test materials in the high relative humidity enclosure.

Test Material	Initial Moisture (wt%)	Measurement Method	Moisture Added (wt%)	Total Moisture (wt%)	Ratio of Water to Metal Cation
Base	0.01	200 °C wt. loss	0.04	0.05	0
Low Ca	0.04	200 °C wt. loss	0.24	0.28	7.28
Low Mg	(0.04)	Est. from Low Ca	0.24	0.29	6.75
High Ca	0.03	TGA	0.36	0.40	1.11
High Mg	0.09	TGA	0.46	0.56	1.58
PMAXBS	0.02	200 °C wt. loss	0.07	0.09	2.90

Table 7 summarizes the conditions inside the enclosure during humidification. The enclosure temperature and relative humidity measurements below are representative of the material in thermal equilibrium with the glovebox. The relative humidity was measured with a probe placed near the top of the enclosure. Temperatures were measured outside the enclosure, inside the enclosure at the location of the relative humidity probe, under the material pan, and in the center of the material. It was evident from the moisture addition results that liquid phases were present in some of the materials, based on the ratio of water to metal cation. The distribution of the liquid phases depends on the relative humidity at various regions within the material. The relative humidity at various regions in the material was calculated, based on the assumption of constant vapor pressure throughout the enclosure. Using this approach, the water vapor pressure was calculated at the location of the sensor. The relative humidity in the material was calculated as the ratio of the vapor pressure inside the enclosure to the saturation vapor pressure at a known temperature in the material. The results of these calculations show that liquid phases would be present throughout the Low Ca test material. The Low Mg, High Ca, and PMAXBS test materials would have liquid phases in cooler regions near the surface, because the thermal gradients would limit moisture adsorption in the interior. The High Mg test material would not have liquid phases.

Table 7. Relative humidity and temperatures within the high relative humidity environment during exposure of the test materials.

Test Material	Total Moisture (wt%)	Exposure Time (hr)	Enclosure Temp (ºC)	Enclosure RH_{max}%	Under Pan TC Temp (ºC)	Material TC Temp (ºC)	Calc. RH% in Material
Base	0.05	137.9	26	56.0	--	39	26.9
Low Ca	0.28	43.0	26	52.6*	41	--	22.7*†
Low Mg	0.29	20.0	26	51.7*	47	47	16.4
High Ca	0.40	21.0	26	30.0*	41	47	9.5
High Mg	0.55	16.8	24	8.0	41	43	2.8
PMAXBS	0.09	107.0	27	53.0*	36	40	25.6

*Indicates that liquid phases may be present due to the deliquescence of calcium or magnesium chlorides at the given temperature and relative humidity.

†Based on material temperature measured under the pan.

After the moisture addition, the test materials were poured into the instrumented 3013 containers and sealed. The process of pouring the material provided a partial mixing of the materials and distributed the liquid phases (if present) throughout the container. The containers were installed on the surveillance rack without insulation for a period of one to three weeks. The relative humidity was measured with a Sensirion sensor placed in the container headspace, immediately below the lid of the container. Temperatures were measured in the container headspace, in the center of the container, under the bottom of the container (outside), and on the outside sidewall three-quarters of the way down from the top. The temperature and relative humidity measurements taken during this period and shown in Table 8 are representative of conditions inside a bare 3013 container prior to placement in a 9975 shipping container.

Table 8. Relative humidity and temperatures within the sealed, uninsulated, instrumented 3013 containers.

Test Material	Total H_2O (wt%)	Sensirion Headspace Temp (ºC)	Headspace relative humidity%	Warmest Measured Temp (ºC)	Location	Calc. RH% in Material
Base[a]	0.05	30	37	34	Can Bottom TC	30
Low Ca	0.28	31	50*	42	Can Bottom TC	27*
Low Mg	0.29	38	37*	46	Can Bottom TC	24
High Ca	0.40	41	18*	43	Can Bottom TC	17*
High Mg[b,c]	0.55	33	0	38	Headspace TC	0
PMAXBS[a]	0.09	36	23*	44	Headspace TC	15*

*Indicates that liquid phases may be present due to the deliquescence of calcium or magnesium chlorides at the given temperature and relative humidity.

[a] Material TC not working.

[b] Temperature measurements for the High Mg test material were not available on day 5 due to instrumentation issues; therefore measurements at day 20 are reported instead.

[c] Can bottom TC not working.

We had expected that the coolest temperatures would be measured in the container headspace and the warmest temperatures would be measured in the material. However, the measurements show that the cooler regions tend to be the headspace and container wall, and the warmest locations tend to be the can bottom. There are several reasons for these observations. First, temperatures given by the material TC (center of container) may be biased low. The 3013 test containers were designed with the material TC in the center of the container, but because the containers with test materials I through V are only half full, the material TC is either above or just touching the surface of the material. Second, the location of a container in the array and the location of the sidewall TC with respect to the other containers in the array may affect the results.

The relative humidity at various regions in the material was calculated, based on the assumption of constant vapor pressure throughout the container. Using this approach, the water vapor pressure was calculated at the location of the sensor. The relative humidity in the material was calculated as the ratio of the vapor pressure measured in the headspace to the saturation vapor pressure at the warmest measured temperature in the container. The results of these calculations show that conditions inside the containers with the Low Ca, High Ca, and PMAXBS test materials support liquid phases throughout the container. Conditions inside the container with the Low Mg test material would support liquid phases, but they would be restricted to cooler regions near the surface. Conditions inside the container with the High Mg test material would not support liquid phases.

Insulation was placed on the containers within one to three weeks after installation. The headspace temperature and relative humidity measurements for the insulated containers from the Sensirion sensors are shown in Table 9. These data, taken 30 days from the date the container was installed on the surveillance rack are representative of the conditions inside 3013 containers after placement inside 9975 shipping containers. The insulation has the effect of increasing the container temperatures and decreasing the relative humidity. The relative humidity at various regions in the material was calculated, based on the assumption of constant vapor pressure throughout the container. Using this approach, the water vapor pressure was calculated at the location of the sensor. The relative humidity in the material was calculated as the ratio of the vapor pressure measured in the headspace to the saturation vapor pressure at the warmest measured temperature in the container. The results of these calculations show that likewise to the bare 3013, conditions inside the containers with the Low Ca, High Ca, and PMAXBS test materials support liquid phases throughout the container. Conditions inside the container with the Low Mg test material would support liquid phases, but they would be restricted to cooler regions near the surface. Conditions inside the container with the High Mg test material would not support liquid phases.

Table 9. Relative humidity and temperatures within the sealed, insulated, instrumented 3013 containers approximately 30 days after installation.

Test Material	Total H_2O (wt%)	Sensirion Headspace Temp (ºC)	Headspace relative humidity%	Warmest Measured Temp (ºC)	Location	Calc. RH% in Material
Base	0.05	36	28	40	Material TC	24
Low Ca	0.28	39	33*	45	Can Bottom TC	24*
Low Mg	0.29	46	27[†]	53	Can Bottom TC	19
High Ca	0.40	43	18*	45	Can Bottom TC	17*
High Mg	0.55	33	0	43	Can Bottom TC	0
PMAXBS[a]	0.09	48	21*	55	Headspace TC	15*

*Indicates that liquid phases may be present based on temperature, relative humidity, and salt composition.

[†] At the lowest temperature of 36°C measured at the container sidewall, the relative humidity is 46%. Magnesium chloride can form liquid phases under these conditions.

[a] Material TC not working.

Conclusion

A series of Pu-bearing test materials containing high and low concentrations of magnesium and calcium chloride salts has been loaded in full-scale tests (instrumented 3013 containers with 2,500 g of material). The test materials have been exposed to a moist air atmosphere to simulate conditions in the Hanford C-line gloveboxes. The Low Ca, Low Mg, High Ca and PMAXBS test materials are inferred to have formed liquid phases, based on the total weight gain, the hydration properties of the AEC salt components present in the materials, and the conditions to which the materials were exposed. The conditions inside the 3013 containers in which these materials were loaded continued to support the formation and persistence of liquid phases during storage. However, liquid phases would not form in the High Mg test material, based on the low relative humidity during exposure and storage.

The weight gain profiles show that materials with magnesium chlorides adsorb moisture at a faster rate than materials with calcium chlorides with the same salt concentration. However, both the Low Mg and Low Ca test materials reached equilibrium below the 0.5 wt% moisture limit in approximately 20 to 30 hours, and both materials had water to metal cation ratios greater than 6. The High Ca and High Mg test materials could reach the 0.5 wt% moisture limit in less than one day. The water to metal cation ratios for these materials were less than 6, and the moisture in the materials did not reach equilibrium with the moisture in the enclosure.

Temperature gradients have a larger effect on the rate of hydration for materials with low salt concentrations. In these materials, the salt components near the surface of material saturate and further hydration does not occur until the interior of the material reaches the critical relative humidity for hydration. The materials with high salt concentrations had nearly constant rates of moisture sorption. Sorption on these materials occurred mostly on or near the surface, which was evident from the top layer of the High Ca material in the pan having a darker appearance than the material beneath the surface. However, we speculate that this effect was a result of the material's high affinity for water limiting the transport of the available moisture through the material.

We infer from this experiment that the Hanford materials exposed to high relative humidity environment (14 to 56%) for periods of hours to days prior to packaging in 3013 containers could also have formed liquid phases below the 0.5 wt% limit for moisture. Formation of liquid phases would be favored in materials with calcium chlorides, which deliquesce at lower relative humidity than magnesium chlorides. Thermal gradients in the material may result in an uneven distribution of moisture, with the liquid phases forming in cooler regions of the material in the pan. The moisture would be redistributed when materials are placed in the container and as the thermal equilibrium is established in the container. Although the relative humidity inside the sealed 3013 containers would be expected to decrease with time in storage, liquid phases could persist inside the sealed 3013 containers, particularly in materials with calcium chlorides.

References

1. Assistant Manager Nuclear Material Stabilization *Integrated Surveillance and Monitoring Program for Materials Packaged to Meet DOE-STD-3013*; AMNMS-15-0014; Department of Energy Savannah River: Aiken, SC, 2015.
2. U. S. Department of Energy *Stabilization, Packaging, and Storage of Plutonium-Bearing Materials*; DOE-STD-3013-2012; Washington, D.C., 2012.
3. U. S. Department of Energy, Stabilization, Packaging, and Storage of Plutonium-Bearing Materials. Washington, D.C., 2004.
4. U. S. Department of Energy, Stabilization, Packaging, and Storage of Plutonium-Bearing Materials. Washington, D.C., 2000.
5. Lillard, R. S.; Worl, L. A.; Veirs, D. K.; Berg, J. M.; Duffey, J. M.; Dunn, K. A.; Livingston, R. R.; Zapp, P. E.; McClard, J. W. *Test plan for determining the susceptibility of 3013 containers to stress corrosion cracking*; LA-UR-09-02953 ; LA-UR-09-2953; 2009.
6. Berg, J. M.; Veirs, D. K.; Kelly, E. J.; Duque, J. G.; Joyce, S. A.; Narlesky, J. E.; Duffey, J. M.; Mickalonis, J. I.; Dunn, K. A. *Test Plan for Assessing Potential for Stress Corrosion Cracking in the 3013 Inner Container Closure Weld Region (FY2014)*; LA-UR-14-20785; Los Alamos National Laboratory: Los Alamos, NM, 2014.
7. Joyce, S. A.; Narlesky, J. E.; Veirs, D. K.; Garcia, E.; Gillispie, O. W.; Jackson, J. M.; Scott, B.; Worl, L. A., Salt phases in calcined materials and their hydration properties. *Journal of Nuclear Material Management* **2010,** *37* (2), 70-80.
8. Greenspan, L., Humidity Fixed Points of Binary Saturated Aqueous Solutions. *Journal of Research of the National Bureau of Standards - A. Physics and Chemistry* **1977,** *81A* (1), 89-96.
9. Washburn, E. W., *International Critical Tables of Numerical Data, Physics, Chemistry and Technology (1st Electronic Edition)*. Online version available at: http://knovel.com/web/portal/browse/display?_EXT_KNOVEL_DISPLAY_bookid=735&VerticalID=0 ed.; Knovel: 1926 - 1930;2003; p 368.
10. Pitzer, K. S.; Oakes, C. S., Thermodynamics of Calcium Chloride in Concentrated Aqueous Solutions and in Crystals. *J. Chem. Eng. Data* **1994,** *39*, 553.

11. Berg, J. M.; Gupta, N. K.; Nguyen, B.; Narlesky, J. E.; Prenger, F. C.; Traver, L. E.; Veirs, D. K., Thermal Gradients and the Potential to Form Liquids in 3013 Containers. *Journal of Nuclear Material Management* **2010,** *37* (3).
12. Boak, J. M.; Eller, P. G.; Erickson, R. M.; Murray, A.; Roberson, G. D. *Technical Basis for Equivalency to DOE Standard 3013 Requirements of Lower-Temperature Stabilization for Electrorefining-Derived Plutonium Oxides, Revision 1*; LA-UR-02-6054; Los Alamos National Laboratory: Los Alamos, NM, 2002.
13. Narlesky, J. E.; Stroud, M. A.; Smith, P. H.; Wayne, D. M.; Mason, R. E.; Worl, L. A. *Characterization of Representative Materials in Support of Safe, Long Term Storage of Surplus Plutonium in DOE-STD-3013 Containers*; LA-UR-12-23790; Los Alamos National Laboratory: Los Alamos, NM, 2012.
14. Gillispie, O. W.; Bender, B. S.; Padilla, D.; Trujillo, L.; Wilson, E.; Maez, R. V. *Surveillance & Monitoring: Preparation and Characterization of Item PMAXBS for Large Scale Surveillance Study* LA-UR-04-1412; LA-UR-04-01412; 2004.
15. Worl, L.; Veirs, D. K.; Lillard, R. S.; Berg, J.; Narlesky, J.; Kelly, E.; Remerowski, M. L.; Dunn, K.; Livingston, R.; Barnes, D. M.; Cheadle, B.; Counts, C.; Loftin, C.; Daugherty, W.; Hackney, B.; Duffey, J.; Zapp, P.; Skidmore, T. E.; Hoffman, E. N.; Paul, T.; Yerger, L.; Venetz, T.; Clarke, S. E. *FY08 surveillance & monitoring program review*; LA-UR-08-00605 ; LA-UR-08-605; 2008.
16. Berg, J.; Garcia, E.; Veirs, D.; Mason, R.; Smith, P.; Remerowski, M. L.; Punjak, W.; Peppers, L.; Narlesky, J.; Duffey, J. M.; Dunn, K.; Shaw, S.; Shepherd, J. E.; McClard, C.; Venetz, T.; Mayhugh, S.; Riley, D.; Roberson, G.; Cheadle, B.; Friday, G.; Paul, T. *FY07 Surveillance and Monitoring Program Review*; LA-UR-07-1371; Los Alamos National Laboratory: 2007.
17. Gillispie, O. W.; Worl, L.; Veirs, D.; Stroud, M. A.; Narlesky, J.; Berg, J.; Kelly, E.; Padilla, D.; Bender, B. S.; Lopez, A. S.; Martinez, M.; Trujillo, L.; Wilson, E. *Preparation and Characterization of a Master Blend of Plutonium Oxide for the 3013 Large Scale Shelf-Life Surveillance Project*; LA-UR-17-22879; Los Alamos National Laboratory: 2017.
18. Worl, L.; Veirs, D.; Padilla, D.; Jackson, J. M.; Lillard, R. S.; Berg, J.; Peppers, L.; Narlesky, J.; Garcia, E.; Joyce, S. A.; Foy, B. R.; Prenger, C.; Stakebake, J. L. *FY07 SURVEILLANCE & MONITORING INTERNAL PROGRAM REVIEW* LA-UR-07-5340; Los Alamos National Laboratory: 2007.

Appendix 1. Overview of the LANL-Produced Materials Used in Previous Full-Scale Tests

PMAXBS

The PMAXBS test material was produced by the MIS program to represent Rocky Flats oxide generated in pyrochemical processes. It was made by blending LANL-produced oxide in the form of burned anode heel with low-purity residue from the electrorefining process containing magnesium chloride.[14] The composition of the PMAXBS test material is given in Table A1-1.

Table A1-1. Plutonium concentration and composition of the Chloride-Salt Components in the PMAXBS test material.

Pu wt%	71.8
Cl ppm (total)	52,000
Cl ppm (leach)	62,000*
Mg ppm (total)	2,400
Mg ppm (leach)	200
Ca ppm (total)	200
Ca ppm (leach)	60
Na ppm (total)	19,000
Na ppm (leach)	19,000
K ppm (total)	35,000
K ppm (leach)	27,000
*The difference between total Cl and soluble Cl is attributed to material inhomogeneity and sampling.	

PMAXBS was initially loaded for 250 days. The moisture content of 0.19% was added by flowing humid gas through the container.[15] After the initial loading, an additional 1.8 g of moisture were added by flowing humid gas through the container, bringing the moisture content to 0.23 wt%. The container was opened 400 days after finding a leak in the container. An inspection of the container revealed corrosion throughout the headspace regions of the container (Figure A1-1). Analysis of the DCB data did not indicate a change. The partial pressure of water vapor in the container at 30 days was 1.0 kPa. The resulting relative humidity was 35% in the headspace and between 8 and 11% in the material.

The PMAXBS test material was reloaded into a second container for 400 days. After opening the second container, slight corrosion was found near the heat affected zones surrounding welds on the container (Figure A1-2). Finally, the material was loaded into a third container. Moisture was added by the material in a closed container with a small dish of water placed on top of the material. The moisture content at the time of loading was 0.4 wt%. The third container was opened 100 days after loading. As in the previous loadings, corrosion was observed throughout the headspace regions of the container (Figure A1-3), and analysis of the DCB data did not indicate a change. The partial pressure of water vapor in the container at 30 days was 3.6 kPa. The resulting relative humidity was at saturation in the headspace and between 27 and 39% in the material.

Figure A1-1. Lid from first modified inner 3013 container loaded with PMAXBS (0.19, 0.23 wt% moisture; 400 days in surveillance). Corrosion observed throughout headspace region.

Figure A1-2. Lid from second modified inner 3013 container loaded with PMAXBS. Container reloaded with PMAXBS (0.23 wt% moisture; 400 days in surveillance) after leak was discovered in first container. Very slight corrosion observed in heat affected zone surrounding weld.

Figure A1-3. Lid from third modified inner 3013 container loaded with PMAXBS (0.4 wt% moisture, 100 days in surveillance). Corrosion observed throughout headspace region.

Masterblend (MB)

A test material called the Masterblend (MB) was prepared following tests with PMAXBS to determine the effect of a corrosive environment on stainless steel inner container lid sections from Lawrence Livermore (316L), Savannah River (304L), Hanford (304L), Rocky Flats (316L), and Los Alamos (316L).[16] In addition, stainless steel DCB specimens of either 304L or 316L were placed in either the headspace or the contact region to determine if the conditions in those locations support crack growth. The MB material was produced by blending LANL-produced oxide in the form burned anode heel with low-purity residue from the electrorefining process.[17] The blended material was spiked with additional 0.75 wt% magnesium chloride in the form of K_2MgCl_4 then calcined to 800°C. The composition of the MB material is given in Table A1-2.

Table A1-2. Plutonium concentration and composition of the Chloride-Salt Components in the MB material.

Pu wt%	63.3
Cl wt% (total)	15 ± 2.5
Mg wt% (total)	0.6
Mg wt% (leach)	0.28
Ca wt% (total)	0.02
Na wt% (total)	3.8
K wt% (total)	6.9

The MB was loaded into 3 full-scale containers. Masterblend container 1 was loaded with 0.3% H_2O, and MB containers 2 and 3 were loaded with 0.45% H_2O.[15] The resulting partial pressure of water vapor in MB containers 1, 2, and 3 measured at 100 days was <0.3 kPa, 0.5 kPa, and 0.5 kPa, respectively. The resulting relative humidity at the coolest region of the containers was < 8% relative humidity in MB container 1 and 14% relative humidity in containers 2 and 3. When the containers were opened, no corrosion was observed on any of the surfaces (Figure A1-3), which is consistent with the relative humidity being below the DRH. These results indicated that the concentration of the AEC salt component in the MB was too high to support corrosion at or below the 0.5 wt% limit in the 3013 standard.

Figure A1-3. Modified inner 3013 container lid showing no corrosion after MB container loading: 105 days in surveillance.

Modified Masterblend (MMB)

The Modified Masterblend was made in an attempt to "blend down" the AEC salt components in the MB by adding higher purity plutonium oxides and produce a material with a similar composition to PMAXBS for an additional three full-scale corrosion tests.[18] The MMB material was prepared by blending 3 parts higher purity oxides produced from recast anode heels, direct oxide buttons, and turnings to 1 part MB material. The ingredients of the MMB are given in Table A1-3.

Table A1-3. Materials Comprising the MMB.

LOT ID	Pu (g)	Net (g)	Pu%
BMB41OXC2	2232	2708.7	82.4
PMA7389OX	582	743.8	78.2
PMA7393OX	751	883.4	85.0
PMA9481OX	987	1239.9	79.6
PMA9524OX	1033	1209.0	85.4
PMB97C10	830	1000.0	83.0
PMB98C11	847	1000.0	84.7
PMB98C12	388	458.4	84.6
	7650	9243.2	82.8
MBCAN4BC (Masterblend)	2527	3988.4	63.4
MMB (total)	10177	13231.6	76.9

The materials were mixed into six, 2-kg batches. Each batch was then blended in a Turbula® mixer. Following blending, the materials were recombined into three batches and calcined to 800°C. Following calcination, the materials were again split into six, 2-kg batches. Each batch was then blended in a Turbula® mixer. Following blending, the materials were recombined back into three batches. The splitting, blending, and recombining process was repeated one additional time. The final composition of the batches is given in Table A1-4. The experiments for which these materials were prepared were never initiated, and the materials were stored and eventually used to prepare the Base Material in the current set of experiments.

Table A1-4. Plutonium Content in the MMB.

LOT ID	Pu (g)	Net (g)	Pu%	mW/g-Net
MBC23B	3336.4	4370.8	76.3	1.81
MBC24B	3255.4	4363.8	74.6	1.79
MBC25B	3238.0	4364.4	74.2	1.81